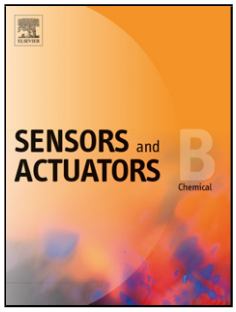

Title: A joint action of aptamers and gold nanoparticles chemically trapped on a glassy carbon support for the electrochemical sensing of ofloxacin

Author: Sanaz Pilehvar Christine Reinemann Fabio Bottari Els Vanderleyden Sandra Van Vlierberghe Ronny Blust Beate Strehlitz Karolien De Wael

PII: S0925-4005(16)31493-9
DOI: http://dx.doi.org/doi:10.1016/j.snb.2016.09.075
Reference: SNB 20940

To appear in: *Sensors and Actuators B*

Received date: 15-6-2016
Revised date: 2-9-2016
Accepted date: 14-9-2016

Please cite this article as: Sanaz Pilehvar, Christine Reinemann, Fabio Bottari, Els Vanderleyden, Sandra Van Vlierberghe, Ronny Blust, Beate Strehlitz, Karolien De Wael, A joint action of aptamers and gold nanoparticles chemically trapped on a glassy carbon support for the electrochemical sensing of ofloxacin, Sensors and Actuators B: Chemical http://dx.doi.org/10.1016/j.snb.2016.09.075

A joint action of aptamers and gold nanoparticles chemically trapped on a glassy carbon support for the electrochemical sensing of ofloxacin

Sanaz Pilehvar[1], Christine Reinemann[2], Fabio Bottari[1], Els Vanderleyden[3], Sandra Van Vlierberghe[1,3], Ronny Blust[4], Beate Strehlitz[2], Karolien De Wael[1,*]

[1] AXES research group, Department of Chemistry, University of Antwerp, Groenenborgerlaan 171, 2020 Antwerp, Belgium

[2] UFZ- Helmholtz Centre for Environmental Research, Department Environmental and Biotechnology Centre, Permoserstrasse 15, 04318 Leipzig, Germany

[3] Polymer Chemistry and Biomaterials Research Group, Ghent University, Krijgslaan 281, 9000 Ghent, Belgium

[4] Sphere Research Group, Department of Biology, University of Antwerp, Groenenborgerlaan 171, 2020 Antwerp

*Corresponding Author: karolien.dewael@uantwerpen.be

Highlights

- A new electrochemical aptasensing strategy is developed based on chemically entrapped AuNPs onto a glassy carbon electrode (GCE) surface for the detection of ofloxacin.
- The covalently anchored AuNPs on the GCE surface were used as electronic bridges, to enhance the probe immobilization capacity and to increase the long-term stability of the attached aptamers.
- The sensor exhibited high specificity toward ofloxacin with a limit of detection (LOD) of 1 nM.
- The developed aptasensing method was successfully applied to determine ofloxacin in tap water and effluent sewage plant water samples.

Abstract

A joint action of ssDNA aptamers and electrochemistry is a key element in developing successful biosensing platforms, since aptamers are capable of binding various targets with high specificity, and electrochemistry is one of the most sensitive techniques for on-site detections. A continuous search for improved immobilization and sensing strategies of aptamers on transducer surfaces resulted in the strategy presented in this article. The strategy is based on the *covalent* attachment of gold nanoparticles on the surface of glassy carbon electrodes through sulfhydryl-terminated monolayer, acting as a glue to connect AuNPs on the electrode. The covalently attached gold nanoparticles modified glassy carbon electrodes have been applied for the efficient immobilization of thiolated ssDNA probes, with a surface coverage of about 8.54×10^{13} molecules cm^{-2} which was 7-fold higher than that on the electrochemically deposited gold nanoparticles. Consequently, improved sensitivity, good reproducibility and stability are achieved for electrochemical aptasensor. Combined with the high affinity and specificity of an aptamer, a simple, novel, rapid, sensitive and label-free electrochemical aptasensor was successfully fabricated for ofloxacin (OFL) detection. The linear dynamic range of the sensor varies between 5×10^{-8} to 2×10^{-5} M OFL with a detection limit of 1×10^{-9} M OFL. A potential application in environmental monitoring was demonstrated by using this sensing strategy for the determination of OFL in (experimentally spiked) real samples such as tap water and effluent of sewage treatment plant. The proposed nanoaptasensor combines the advantages of the covalent attachment of neatly arranged AuNPs (enlarged active surface area and strengthened electrochemical signal) and the elimination of labels for the amplified detection of OFL, with the covalent attachment of highly specific aptamers to the surface of the modified electrode.

Keywords

Ofloxacin; Au nanoparticles; Electrochemical aptasensor; Covalent attachment; Water quality; Environmental monitoring

1. Introduction

The growing use of pharmaceuticals constitutes a public health concern on the presence of these compounds in the environment due to their long-term adverse effects on human health and wildlife [1]. Among different pharmaceutical compounds, antibiotics are of particular concern, as they can induce bacterial resistance, even at low concentrations. After intake, antibiotics undergo metabolic processes in organisms. However, significant fractions of the parent compound are excreted in unmetabolized form or as metabolites into sewage and wastewater treatment systems [2]. It has also been shown that substances of pharmaceutical origin are often not eliminated during wastewater treatment and also not biodegraded in the environment. Although there are no limits for antibiotics in drinking and surface waters until now, the European Union and World Health Organization recommend sparingly and careful use of antibiotics [3, 4]. Consequently, the monitoring of antibiotics residues is of great importance for efficient risk management [1, 5].

Fluoroquinolones (FQ) are important antibacterial agents, having a broad spectrum of activity against both Gram-negative and Gram-positive bacteria [6]. Their molecular structure contains a fluorine at position 6 and a piperazine substituent at position 7 of the naphthyridine ring of quinolones [7]. Ofloxacin (OFL, Figure 1) is considered to be a second generation of FQ's having activity against bacteria through inhibition of DNA supercoiling activity of DNA gyrase [8].

Figure 1

However, it has been shown that 70% of OFL was excreted in unmetabolized form into water environment, leading to negative effects on human health [5]. As a result, many methods have been developed for the determination of OFL, including electrochemical methods [9-16], spectrophotometric methods [17, 18], and chromatographic methods [19, 20]. However, in spite of their high selectivity and sensitivities (LOD of 0.01-16 μg/ml ($\approx 2.7\times10^{-8}$– 4.4×10^{-5} M), these techniques are time-consuming, require complex sample procedures and involve the use of large amounts of reagents and organic solvents thus need considerable costs. Whereas (bio)sensors based on aptamers attract remarkable attention due to their fast response, low cost and high specificity and sensitivity especially when operating with electrochemistry. Aptamers are oligonucleotide sequences selected by the systematic evolution of ligands by exponential enrichment (SELEX) technique and capable of binding with high affinity and specificity to a target molecule [21]. Recently, a group of aptamers was selected with specificity for fluoroquinolones and high affinity for ofloxacin (K_d = 0.1–56.9 nM) [22]. These aptamers were selected experimentally by use of the Capture-SELEX method [23], which is suitable for small molecule targets generating aptamers performing a structure switch caused by target binding. The applicability of these quinolone-specific aptamers was successfully tested in real water samples (e.g. effluents of sewage plants), suggesting they can be used as suitable molecular receptors in biosensors for improved monitoring in real samples such as polluted water. Biosensors based on aptamers as recognition elements offer several advantages of high selectivity, good stability, easy regeneration, and wide applicability [24, 25]. Therefore, a number of aptasensors have been developed in the past decade, including fluorescent [26], colorimetric [27], chemiluminescence [28], electrochemiluminescent [29] and electrochemical aptasensors [30-34] for the sensitive detection of nucleic acids [33], proteins [34, 35], cells [36], small molecules [37, 38] and metal ions [39, 40]. Though all the methods developed could realize the detection of small pharmaceutical molecules successfully, some common disadvantages became clear. For example, most of the existing aptasensing methods require a labeling step, of or the ssDNA molecules or the targets. Such a labeling process would not only make experiments relatively complex and expensive, but might also affect the binding affinity between the targets and their aptamers. In addition, the appearance of pharmaceutical residues in very low concentration levels in the environment increased the demand for ultrasensitive aptadetection.

Bio-functionalized nanomaterials, and especially metal nanoparticles, offer several advantages for signal amplification due to their facile synthesis, large surface area, high chemical stability, biocompatibility, good conductivity, and they can bind to amine or thiol-containing molecules with high affinity. Among different metal nanoparticles, gold nanoparticles (AuNPs) can fulfil the requirement for a sensitive aptasensing device, since they are biocompatible and provide good conductivity [41]. The use of AuNPs for the fabrication of aptasensors may increase the surface area, promotes the binding of ssDNA aptamers on the electrode surface, and therefore improve the sensitivity [41]. Therefore, AuNPs are used extensively in developing optical aptasensors [42], colorimetric aptasensors [43, 44] and electrochemical aptasensors [45, 46]. Recent developments in nanostructured material synthesis have had a huge effect on the design of novel electrochemical transduction systems, thus enhancing the performance of aptasensors based on AuNPs [46-51]. Wei et al. combined two amplification strategies, including a dual signaling strategy and supersandwich assay to fabricate an electrochemical aptasensor for the detection of Adenosine triphosphate [52]. In another study, an electrochemical biosensor is proposed which employs the integration of molybdenum selenide nanoflowers, AuNPs, aptamer and the guanine-rich complementary DNA sequence for the sensitive detection of ochratoxin A [53]. Later on, an electrochemical aptasensor based on target-induced strand displacement and AuNPs amplification was developed for the determination of Salmonella. The aptamer for Salmonella was captured on the sensing interface by hybridizing with a capture probe. In the presence of Salmonella, the aptamer dissociated from the capture probe because of the stronger interaction between the aptamer and the Salmonella [54].

Different methods have been developed to functionalize electrode surfaces with AuNPs including physisorption, electrochemical deposition, and photochemical deposition [55]. Roushani et al. have proposed a nanoaptasensor based on AuNPs, electrochemically deposited on the surface of a glassy carbon electrode for detection of ibuprofen [56]. In this study, ultrasensitive detection of ibuprofen was achieved via deposition of AuNPs

on the surface of a GCE (not covalently anchored) to increase the effective electrode surface and sensitivity and to provide a unique platform for increased loading of aptamers. However, an effective method of functionalization of the electrode surface with AuNPs should lead to a robust system where an optimal electronic coupling between AuNPs and the electrode surface exists [57, 58]. It has been shown that terminating the electrode surface with functionalities, which are able to covalently bind AuNPs, results in a stable thin film of AuNPs on the electrode surface [57, 58]. Inspiringly, we used a sulfhydryl terminated linker to attach AuNPs to the surface of a glassy carbon (GC) electrode. This method has been used for the adsorption of hemoglobin on the surface of a GC electrode by Zhang et al. [59]. However, in this study, for the first time, a covalent binding of AuNPs on the surface of a GC electrode by a sulfhydryl terminated linker is utilized as an efficient immobilization strategy for ssDNA aptamers immobilization. The objective of our work is to evaluate and demonstrate that covalent attachment of AuNPs can be employed for a stable, flexible and repeatable aptamer immobilization and its application for potential sensor development. In addition, no study is reported on the detection of OFL via the use of aptamers and electrochemistry. To realize our design, GC electrodes are first modified with 4-aminobenzoic acid, followed by the introduction of terminal thiol groups by incubating the electrode in a 4-aminothiophenol solution. Subsequently, AuNPs are self-assembled on the surface of the electrode as an immobilization platform for thiolated aptamers. The integrated immobilization technique moved the aptamer into a more solvated environment where more OFL molecules are present. This allows target molecules to interact with immobilized aptamers more efficiently compared to the situation where the aptamers are directly immobilized on the electrode surface [60, 61].

2. Experimental Section

2.1. Chemicals and Reagents

Mercaptohexanol (MCH), hexaammineruthenium(III) chloride (RuHex), and tris(2-carboxyethyl) phosphine hydrochloride (TCEP), hydrogen tetrachloroaurate ($HAuCl_4$), 4-aminothiophenol (4-ATP), 1-ethyl-3-(3-dimethylaminepropyl)-carbodiimide (EDC), aminobenzoic acid (4-ABA) and lithium perchlorate ($LiClO_4$) were purchased from Sigma-Aldrich (Diegem, Belgium). A 20 mM Tris-HCl (tris(hydroxymethyl)aminomethane hydrochloride) solution containing 100 mM sodium chloride (NaCl), 20 mM, 2 mM magnesium chloride ($MgCl_2$) and 1 mM calcium chloride (KCl) (pH 6.6) was used as the immobilization and binding (I-B) buffer. Pefloxacin methylate and chloramphenicol were purchased from Sigma-Aldrich (Diegem, Belgium). Nalidixic acid was purchased from Duchefa Biochemie (The Netherlands). All substances were diluted to a final concentration in I-B buffer (100 mM NaCl, 20 mM Tris–HCl pH 6.6, 2 mM $MgCl_2$, 1 mM $CaCl_2$). The solution of 4-ABA was prepared in acetonitrile (ACN) containing 0.1 M $LiClO_4$. The thiolated OFL binding aptamer Q8 [22] and other DNA oligonucleotide obtained from Eurogentec (Liege, Belgium). The sequences of them are listed as follows:

The thiolated OFL binding aptamer Q8:

(5'-SH-$(CH_2)_6$-ATACCAGCTTATTCAATTAGTTGTGTATTGAGGTTTGATCTAGGCATAGTCAAC
AGAGCACGATCGATCTGGCTTGTTCTACAATCGTAATCAGTTAG-3')

and thiolated 90 mer random oligonucleotide:

(5'-SH-$(CH_2)_6$-NNNNNNNNNNNNNNNNNNNNNNNNNNNNNNNNNNNNNNNNNNNNNNNNNNNNNNN
NNNNNNNNNNNNNNNNNNNNNNNNNNNNNNNNNNN-3')

All oligonucleotide stock solutions (1×10^{-5} M) were prepared with I-B buffer solution (pH 6.6)

To evaluate the applicability of the aptasensor, detections were performed in local tap water (UA, Antwerp, Belgium) as well as in real samples collected from effluent of municipal sewage treatment plants (Aartselaar, Belgium), which receive water from hospitals in Antwerp, Belgium. The effluents of sewage plant and tap water samples were collected in amber glass bottles and stored in the dark at 4°C until analysis. All the samples were vacuum-filtered through a 0.20 μm filter to remove suspended matter, and the sample pH was adjusted to 6.6 with I-B buffer solution (2:1). Calibration curves for quantification were produced by spiking the water samples with OFL at different concentrations. All other reagents were of analytical quality and milli-Q water was used for all aqueous solutions and rinsing.

2.2. Preparation of Aptamer Modified GC Electrode (APT/AuNPs/ATP/ABA/GCE)

AuNPs were prepared according to the procedure described in literature, i.e. a chemical reduction procedure [62]. Briefly, the solution of 0.01% $HAuCl_4$ was stirred and heated up to 100 °C. An amount of 1% sodium citrate solution was immediately added to 100 mL of $HAuCl_4$ solution under stirring. The solution color turned from clear liquid to wine red and was cooled to room temperature with continuous stirring. The solution of gold nanoparticles (average diameter of ca 15 nm) was kept at 4°C and protected from light [62].

Next, the GC electrodes were polished both with fine emery paper and with 1 and 0.05 μm alumina slurry on microcloth pads followed by cleaning in an ultrasonic bath. The cleaned GC electrode was treated using cyclic voltammetry and swept in the potential range of -1.0 until +0.8 V at 50 mVs^{-1} for 8 cycles in a 1.0×10^{-3} M 4-ABA solution (ACN, 0.1 M $LiClO_4$) (ABA/GCE) to form a carboxyl-terminated monolayer (ABA/GCE). The 4-ABA modified GCE thoroughly rinsed with ethanol and distilled water to remove any physisorbed and unreacted materials from the electrode surface. Then, the 4-ABA modified GCE was immersed into aqueous/ethanol (1:1, v/v) solution of 1×10^{-4} M EDC and 1×10^{-4}

M 4-ATP for 1 hr to prepare a well-assembled thiol monolayer on the electrode surface. The electrode modified with ABA and ATP was subsequently washed with ethanol and doubly distilled water to remove the unreacted reagents (ATP/ABA/GCE). Then, it was immersed in a colloidal gold solution for 8 hr at 4°C, during this step gold nanoparticles attach to the sulfhydryl terminated linker on the surface of electrode to obtain the gold nanoparticles modified GCE (AuNPs/ATP/ABA/GCE). In the next step, an 8 µL droplet of OFL binding aptamer solution (2.5×10^{-6} M) was placed on the AuNPs/ATP/ABA/GCE electrode surface during 12 hr at 4°C. After being washed with the I-B buffer, the electrode was incubated for 30 min in 1×10^{-3} M MCH to fill any unoccupied gaps on the gold nanoparticle modified surface, in order to prevent subsequent non-specific adsorption (APT/AuNPs/ATP/ABA/GCE). For target OFL detection, 10 µL of OFL solution with a certain concentration was placed onto the sensing interface to incubate for 2 hr at room temperature after rinsing with the I-B buffer.

2.3. Instrumentation and measurement procedures

The chemical composition of the different electrode surfaces was determined using FISONS S-PROBE, X-ray photoelectron spectroscopy instrument (XPS), by means of the fine focus Al-Ka source with a quartz monochromator, developed by Fisons Instruments Surface Science ensures lower background and higher sensitivity than conventional twin anode sources. The measured spectrum was displayed as a plot of the number of electrons (electron counts) versus electron binding energy in a fixed, small energy interval. Cyclic voltammetry (CV), differential pulse voltammetry (DPV), electrochemical impedance spectroscopy (EIS), and chronocoulometry (CC) were performed with a PGSTAT20 µAutolab Type III potentiostat controlled by Nova 1.9 software package equipped with FRA2 (ECO Chemie, Utrecht, The Netherlands). A conventional three-electrode cell was employed enclosing a bare GC working electrode (BASi®, 3 mm in diameter), a GC counter electrode (Metrohm), and an Ag/AgCl reference electrode filled with saturated KCl solution (Metrohm, Belgium). All the potentials in this paper are given with respect to Ag/AgCl. EIS experiments were performed in 0.1 M KCl solution containing 1×10^{-3} M $K_3[Fe(CN)_6]/K_4[Fe(CN)_6]$ (1:1). The impedance measurements were performed at an open circuit potential of 0.17 V within the frequency range of $1–10^5$ Hz. Scanning electron microscopy (SEM) images were taken using a QuantaTM 250 FEG (FEI, Eindhoven, The Netherlands). The DPV measurements were performed from -0.1 to 0.6 V (interval time = 0.017 s; step potential = 5 mV; modulation amplitude = 50 mV). UV-visible spectra was recorded using a double beam Cary 100 UV-Vis spectrophotometer (Varian Inc. USA).

3. Results and Discussion

3.1. Design strategy of the AuNPs-based aptasensor

A schematic representation of the stepwise procedure of the modification of the electrode for OFL aptasensing is given in Scheme 1. The biosensor was fabricated by electrodeposition of 4-ABA and self-assembly of 4-ATP for the covalent attachment of AuNPs [57]. In the next step, a 5′-thiol-modified OFL-aptamer Q8 was immobilized on the electrode surface via sulfur-gold affinity and then backfilled with MCH to prevent any non-specific adsorption. In the absence of the target, the ssDNA aptamer modified electrode resulted in a very low background voltammetric signal. Caused by target binding, a conformational change of ssDNA aptamers occurred which forced OFL molecules close to the surface of electrode, enabling an efficient electron transfer process between OFL molecules and the transducer surface [59].

Scheme 1

To elucidate the electrode reaction of OFL, repetitive CV scanning of the bare GCE in the 5×10^{-5} M OFL were performed (Supplementary Information, Figure S1). In the cyclic voltammogram, the oxidation peak was observed on the anodic branch around +0.92 V (vs. Ag/AgCl) explained as the irreversible oxidation of the piperazine moiety of the OFL molecule (Figure 1) [63]. The anodic current for OFL oxidation decreases with increasing the potential scan rate, reaching a constant value after 10 scans. This may suggest that most of the OFL molecules are consumed during the initial scans, followed by the electrode surface blockage by products of electro-oxidation of OFL, which blocks the further mass transportation and electron transfer of OFL. In addition, scan rate studies were carried out to study the nature of the electrochemical reaction of OFL at a glassy carbon electrode (Supplementary Information, inset of Figure S1). The oxidation current of OFL was observed to increase with scan rate due to heterogeneous kinetics. The relationship between the logarithm of the peak current and the logarithm of the scan rate showed a straight line with the equation of $y = 0.46x+0.086$. A slope of 0.46 is close to the theoretical slope of 0.5 for a diffusion-controlled process where the OFL species diffuse from the bulk solution to a planar electrode surface. Furthermore, the peak potential (E_p) of the oxidation process was dependent on the scan rate showing the irreversibility of the OFL oxidation reaction [64, 65].

3.2. Characterization of the AuNPs-based aptasensor

3.2.1. SEM, XPS and CV

A SEM examination of the AuNPs/GCE shows round-shaped bright spots, which can be assigned to the presence of gold nanoparticles on the electrode surface (Fig. 2A). The influence of the AuNPs deposition method on the electrode surface morphology has been investigated. The obtained SEM images clearly show that the aggregation of gold nanoparticles did not occur during modification of ATP/ABA/GCE with AuNPs by covalent attachment. In this case, the particles are evenly and homogeneously distributed on the surface of the electrode with particle sizes of 15-20 nm (Fig. 2A, b). The functional groups present on the electrode surface may control the lateral interactions between the nanoparticles and separate the individuals [66, 67]. On the other hand, when AuNPs are only physically deposited on the surface of a GCE, aggregation of AuNPs on the surface is observed (Fig. 2A, c). These results show the positive effect of covalent binding of AuNPs on the morphology of the surface, which might also influence the performance of the aptasensor [59].

The attachment of 4-ABA, 4-ATP and AuNPs to the surface of a GCE has proven by XPS analysis, as shown in Fig. 2B (i), (ii), (iii) and (iv). As illustrated in Fig. 2B (i), the characteristic N(1s) band located at 399 eV appeared after electrodeposition of 4-ABA, showing that 4-ABA has been grafted onto the GCE surface [68]. The binding energy of 399 eV ascribes to the formation of a carbon-nitrogen bond between amine cation radicals and aromatic moiety of the GCE [68]. The attachment of 4-ATP to the surface of the 4-ABA/GCE has been proven by the appearance of the S(2p) band at 165 eV (Fig. 2B, ii) [59]. The XPS spectrum for the AuNPs/GCE contains Au(4f) at 88 and 84 eV, which confirms the successful deposition of the gold nanoparticles on the surface of the ATP/ABA/GCE (Fig. 2B, iii) [59]. In addition, the grafted AuNP film was found to be very stable, since the XPS signal for Au(4f) is still remarkable after ultrasonic rinsing of the AuNPs/ATP/ABA/GCE (Fig. 2B, iv).

The electrochemical stability of AuNPs/ATP/ABA/GCE and a AuNPs/GCE was studied by CV in a 0.1 M KCl solution at 0.05 V s^{-1} [57]. As shown in Fig. 2C, the appearance of the oxidation peak around +1.01 V and a second reduction peak around +0.52 V proves the existence of AuNPs on the surface of the electrode. However, these two peaks disappear with increasing scan numbers, indicating that the nanoparticles, which are only physically adsorbed on the electrode can be stripped off easily by electrochemical cycling. Fig. 2C depicts a well-defined anodic peak at the AuNPs/ATP/ABA/GCE (solid line, curves 1, 2), even after five successive scans, providing evidence for a robust linkage of AuNPs to the surface. In contrast, the peaks related to the gold nanoparticles at the AuNPs/GCE (dashed lines, curves 3,4) are almost diminished after successive scans, suggesting the weak linkage between gold nanoparticles and the electrode surface [75]. The charge related to the oxidative peak for AuNPs/ATP/ABA/GCE and AuNPs/GCE was determined to be $160.63\pm9.41\times10^{-6}$ C and $4\pm1.4\times10^{-9}$ C, respectively. The higher charge value obtained at the AuNPs/ATP/ABA/GCE shows the efficient deposition and higher amount of AuNPs on its electrode. [70, 71].

Figure 2

3.2.2. EIS and CC

Figure 3 shows the Nyquist plots of the impedance spectra obtained at each preparation step, recorded in a 0.1 M KCl solution containing 1×10^{-3} M $K_3[Fe(CN)_6]/K_4[Fe(CN)_6]$. The obtained impedance spectrum allows us to monitor the changes in the interfacial properties of the modified electrodes such as capacitance or electron-transfer resistance. This analysis is achieved by translating the impedance spectrum into an equivalent circuit, commonly consisting of resistances and capacitances representing the different electrochemical and physiochemical properties of the electrodes under analysis. The most frequently cited equivalent circuit used to interpret electrochemical impedance spectra is the Randle's equivalent circuit as shown in the inset of Fig. 3. It shows solution resistance (R_s) in series to a parallel combination of double layer capacitance (C_{dl}) to the charge transfer resistance (R_{ct}) in series with a Warburg impedance (W). The bare GCE exhibits a very small semicircle domain (R_{ct} = 60 kΩ), suggesting a very low electron transfer resistance to the redox couple $Fe(CN)_6^{3-}/Fe(CN)_6^{4-}$ dissolved in the electrolyte solution (curve 1). After the electrodeposition of 4-ABA, the diameter of the semicircle increased dramatically and the change in the R_{ct} was about 300 Ω (curve 2). This observation can be explained by the presence of the acid groups on the 4-ABA monolayer, which are negatively charged and block the electron transfer of the redox couple $Fe(CN)_6^{3-}/Fe(CN)_6^{4-}$ [72]. When 4-ATP is self-assembled on the 4-ABA modified GCE, the R_{ct} decreased dramatically with a value of about 240 Ω (curve 3). In this case, the carboxylic acid groups of 4-ABA are tagged with activated amines of 4-ATP [73]. Curve 4 in Fig. 3 shows a very small semicircle and the R_{ct} decreased with a value of about 100 Ω when AuNPs were self-assembled on the surface of the ATP/ABA/GCE, attributable to the fact that AuNPs can further enhance the electron transfer rate and can lead to the increased effective surface area of the electrode. When ssDNA aptamers were bound on the surface of the AuNPs/ATP/ABA/GCE, the R_{ct} markedly increased with a value of 150 Ω (curve 5), which is due to the created kinetics barrier between $Fe(CN)_6^{3-}/Fe(CN)_6^{4-}$ and the negatively charged phosphate backbones of the aptamer [74]. After the treatment of APT/AuNPs/ATP/ABA/GCE with MCH, the R_{ct} increased with a value of about 100 Ω (curve 6), which is the result of the more complete coverage of the electrode by MCH [75]. The fitted data for the elements used in the equivalent circuits are presented in the Table 1. The quality of fitting to equivalent circuit was judged by the chi-square value (χ^2). These results with low values of Chi square ($<1\times10^{-3}$) indicate that the experimental data were confirmedly fitted with equivalent circuits.

Figure 3

The surface density of the immobilized ssDNA probe was measured from the redox charges of $[Ru(NH_3)_6]^{3+}$ electrostatically associated with the negatively charged backbone of the aptamer by the CC methods [76]. The amount of electroactive oligonucleotides on the electrode surface (Γ_{DNA}) was calculated based on the following equations:

$$\Gamma_{Ru} = \frac{Q}{nFA} \quad \text{(Equation 1)}$$

$$\Gamma_{DNA} = \Gamma_{Ru} \frac{z}{m} N_A \quad \text{(Equation 2)}$$

where Γ_{Ru} is the surface concentration of $[Ru(NH_3)_6]^{3+}$, Q is the charge corresponding to $[Ru(NH_3)_6]^{3+}$ electrostatically bound to surface-confined ssDNA, N_A is Avogadro's number, n is the number of electrons transferred in the reaction (n=1), F represents the Faraday constant, A is the effective surface area of gold electrode (cm^2), z is the charge of the redox molecules, and m is the number of nucleotides in the DNA.

The density of ssDNA immobilized on the AuNPs/AuNPs/ATP/ABA/GCE electrode (Γ_m) is calculated to be $8.542\pm0.54\times10^{13}$ molecules cm^{-2} when a concentration of 2.5×10^{-6} M of aptamers solution is used. The total amount of ssDNA probes immobilized on AuNPs/ATP/ABA/GCE is seven fold higher than that obtained by Lia et al. from the AuNPs modified GC which is prepared by the electrochemical deposition of nanoparticles (AuNPs/GCE) (1.2×10^{13} molecule cm^{-2}) [77]. It confirms that the covalent binding of AuNPs increases the amount of immobilized aptamers, and thus, aptasensors with AuNPs modification can capture more target molecules and accumulate them on the electrode surface, resulting in signal amplification for OFL detection.

3. 3. Performance of the AuNPs-based aptasensor

3.3.1. Electrochemical aptasensing of OFL

To understand the interaction between the aptamer Q8 and the target molecule OFL, the aptamer modified electrode (APT/AuNPs/ATP/ABA/GCE) was incubated with OFL molecules followed by CV analysis (Fig. 4A). As shown in Fig. 4 a (curve 4), a well-defined anodic peak around +0.90 V (vs. Ag/AgCl) appears when the APT/AuNPs/ATP/ABA/GCE was incubated with OFL (5×10^{-5} M), even after being rinsed [78]. A same amount of OFL was exposed to several electrodes, i.e. bare GCE, ABA/GCE, ATP/ABA/GCE and AuNPs/ATP/ABA/GCE (all without aptamer modification). No typical oxidation process, linked to the presence of OFL, could be detected at the bare GCE (Fig. 4A, curve 1), ABA/GCE (Fig. 4B, curve 3), ATP/ABA/GCE (Fig. 4B, curve 4) or AuNPs/ATP/ABA/GCE (Fig. 4A, curve 2). In contrast, the oxidation peak related to the OFL clearly appears when an aptamer modified electrode (APT/AuNPs/ATP/ABA/GCE) is incubated with OFL solution (5×10^{-5} M). The presence of the OFL-related peak at the APT/AuNPs/ATP/ABA/GCE and the absence of this peak at the ABA/GCE, ATP/ABA/GCE and AuNPs/ATP/ABA/GCE (after washing) show that the capturing effect takes place only at aptamer modified electrodes. The specific interaction between aptamer and target molecules of OFL may results in the efficient transfer of the analyte molecules from bulk solution to the electrode surface, leading to easy electron transfer between the electroactive OFL molecules and the electrode surface [75, 79].

Figure 4

Earlier studies demonstrated that SAMs of short-chain alkanethiols could be electrochemically desorbed from gold surfaces through the cleavage of the sulphur-gold bond. In order to test the stability of an APT/AuNPs/ATP/ABA/GCE after the electrochemical detection of OFL, the reductive desorption of thiolated ssDNA from the gold electrode surface has been performed in a 0.5 M NaOH solution after aptadetection of OFL (Supplementary information. Fig. S2). The obtained cyclic voltammograms showed the typical thiol reductive peak to be around -0.9 and -1.1 V, suggesting the presence of ssDNA, even after being used for the detection of OFL [80]. It is worth mentioning that the peak current related to OFL disappeared after the reductive desorption of the thiolated aptamer from the electrode surface. This implies the efficiency of the developed immobilizing strategy to form a stable ssDNA aptamer monolayer onto the electrode surface.

3.3.2. Optimization of the experimental conditions for the electrochemical detection of OFL at APT/AuNPs/ATP/ABA/GCE

To ensure the best performance of the biosensing system, the pH of the electrolyte solution was optimized (Fig. 5A). Therefore, the electrochemical responses of OFL dissolved in buffer solutions with different pH were measured at APT/AuNPs/ATP/ABA/GCE. As shown in Fig. 5A, the electrochemical response of OFL initially increased with the increasing solution pH value to pH 6.5, and then decreased/stabilized decrease between pH 6.5 and 8.5. This can be due to hydrolysis, occurring at increased pH values, leading to changes in the structure of the OFL molecules and dissociation of the aptamer-OFL complex [81]. Another reason might be an increased concentration of hydroxyl ions surrounding the OFL molecules, which creates repulsive forces between the negative phosphate backbone of the aptamer and OFL molecules. The highest current response for OFL was obtained in the buffer solution at pH 6.6. Therefore, pH 6.6 was selected to perform further experiments. Moreover, E_p and solution pH show a linear relationship with a regression equation of E_p= 1.164-0.044 pH. The slope of 0.044 V/pH indicates that the numbers of proton and electron transferred is equal.

Figure 5

The dependence of the incubation time of APT/AuNPs/ATP/ABA/GCE with OFL solution on the DPV oxidation peak of OFL (1×10^{-6} M) was studied and optimized (Fig. 5B). The peak current increased with increasing incubation time up to 120 min (0.14×10^{-6} A) and then decreased at 220 min (0.09×10^{-6} A). This can be due to the fact that the incubation time higher than 120 min causes a saturation on the sensor surface where dissociation of target–aptamer complex from an electrode surface is likely to occur [82]. Thus, 2 hr was chosen as the optimum incubation time. Moreover, the effect of the ssDNA concentration on the performance of the sensor was explored by measuring the impedance signal of the electrode modified by different concentrations of aptamer (5×10^{-9}- 5×10^{-6} M) (Fig. 5C). When the concentration of the aptamer solution has been set to 5×10^{-9} M, the resulting impedimetric signal change (ΔR) after incubation of the aptamer modified electrode with OFL ($\Delta R=R_{ssDNA/OFL}-R_{ssDNA}$) was 20 Ω. The largest impedimetric signal change (ΔR=80 Ω) obtained at the concentration of 2.5×10^{-6} M for aptamers. The impedimetric signal decreased to 40 Ω when the concentration increased to 5×10^{-6} M. A steric hindrance or electrostatic repulsion between negatively charged DNA molecules at higher concentrations might explain the decrease in the impedimetric signal [83]. For this reason, the optimum DNA concentration was adopted for the 2.5×10^{-6} M of aptamer.

3.3.3. Selectivity, reproducibility and stability of the aptasensor

To evaluate the selectivity of the proposed aptasensor toward its target analyte (OFL), three antibiotics including chloramphenicol (CAP) (phenicols), nalidixic acid (NAL) (quinolones) and pefloxacin (POFL) (quinolones) were chosen. The ability of the aptamer to bind selectively with fluoroquinolones in comparison to other antibiotics was previously studied and confirmed [22]. As shown in Fig. 6, a significant increase in the DPV signal at +0.90 V (vs. Ag/AgCl) induced by the interaction of the aptamers with OFL (1×10^{-6} M) was observed. The change in the oxidation peak current (ΔI) at +0.90 V at APT/AuNPs/ATP/ABA/GCE was 0.14×10^{-6} A (column a), which was much higher than that of the other quinolones for the same concentration: 0.045×10^{-6} A for POFL (column d), 0.024×10^{-6} A for NAL (column c) and 0.015×10^{-6} A for CAP (column b), respectively. Besides, the same binding affinity for POFL and OFL was observed during selection process for the aptamer Q8 which explains the obtained electrochemical response for POFL during the electrochemical detection. Furthermore, it was observed that the oxidation peak current of OFL (1×10^{-6} M) decreased only about 5% in the presence of CAP (1×10^{-5} M), NAL (1×10^{-5} M) and POFL (1×10^{-5} M) in the solution (compared to the peak current when only OFL present in the solution). In other experiments, the selectivity of the aptamer in the presence of OFL was analyzed and compared with signals derived from experiments employing random control ssDNA primers. The results show that while there is a remarkable change in DPV response when OFL binding aptamer modified GCE is incubated with OFL (1×10^{-6} M) (column a), a smaller change in current is recorded at the random primer ssDNA modified electrode (column e). This result indicates that almost no interaction between the control DNA and OFL is detectable.

Figure 6

The reproducibility of the designed aptasensor was investigated with inter-assay precision by measuring the same concentration of OFL by five independently prepared electrodes under the same experimental conditions. The relative standard deviation (RSD) of the inter-assay is calculated to be 3.7%, suggesting good reproducibility of the aptasensor. The designed aptasensing interface could be regenerated by immersion in hot water. The signal response recorded by CV recovered up to ~85% of the original signal response. The current response to OFL lost ~15% after each regeneration of the electrode. The storage stability of the aptasensor is one of the key factors in its application and development. The long-term stability of the aptasensor was studied for seven, 14- and 21-day periods. After keeping aptamer modified electrodes in refrigerator (4°C), the aptasensor was used to detect the same OFL concentration (1×10^{-6} M). The response current retained 97%, 93% and 88% of its initial response after 7, 14 and 21 days, respectively, demonstrating the aptasensor's storage capabilities. This might be attributable to the fact that the covalent attachment of AuNPs on the surface of the GCE may provide a suitable biocompatible microenvironment for aptamer immobilization in order to stabilize their activity.

To demonstrate the accuracy of the designed electrochemical method, the detection results were compared with those of a UV spectrophotometric method. Three different concentrations of OFL spiked plant sewage and tap water samples were analysed by the electrochemical method (DPV) and by UV-Vis spectrophotometer and the obtained results are shown in Table 2. The recovery values for both methods are very close to the concentrations of the standard samples, indicating that both methods have good accuracies. The obtained RSD values for the electrochemical aptasensor, which ranged from 1.12% to 6.73%, is slightly higher than that for UV-Vis method (0.55–4.83%). However, the electrochemical aptasensor is superior with respect to its much lower detection limit and selectivity.

3.3.4. Linear range, limit of detection and real sample analysis

The detection performance of the developed aptasensor was evaluated by exposing the aptasensor to a series of OFL concentrations and measuring the resulted DPV signal. The plot of the DPV response as a function of OFL concentrations is illustrated in Fig. 7. It was observed that the increase in OFL concentration induces an increase in DPV signal. The value of ΔI is linearly related to the OFL concentration in the range of 5×10^{-8} M to 2×10^{-5} M. The calibration equation was $\Delta I = 0.0382C + 0.0905$ with a correlation coefficient of 0.9874. The calculated detection limit is 1×10^{-9} M based on three times standard deviation of the blank divided by the slope of the calibration curve ($3\sigma/m$). The limit of detection for the OFL was calculated to be 1×10^{-9} M. The results indicate that the present method can successfully detect OFL with high sensitivity and low detection limit (Table 3). The high sensitivity of the designated aptasensor is owned to the high affinity of Q8 aptamers toward OFL molecules ($K_d=0.2\times10^{-9}$ M) and the efficient immobilization platform construction method which has been integrated. The functionality of the Q8 aptamers in real water samples has been proven positive in former investigations [22]. Here, to demonstrate the practicality of the proposed electrochemical aptasensor, a recovery test was carried out by the standard addition method in tap water and effluent of sewage plant samples. The obtained results are in good agreement with the given concentration with the recovery of 96% for tap water samples and 93.6% for effluent of sewage samples (n=3), whereas the RSD values were below 6.8% (Table 1). This indicates that the developed aptasensor has a promising feature for the practical use in real water samples.

Figure 7

Several studies were performed for the electrochemical detection of OFL (Table 3) [13-19, 78]. Electrochemical biosensing of OFL was first performed by Zhang et al. where an electrochemical immunosensor was developed for OFL detection by employing a polypyrrole film-Au nanoclusters modified GC electrode as a sensor platform and horseradish peroxidase/horseradish peroxidase secondary antibody immobilized on gold nanorods as the detection label [13]. Later on, He et al. reported on the development of an electrochemical immunosensor based on a dual amplification strategy using multiwall carbon nanotubes-poly(l-lysine) as a matrix to immobilize the antigen and multi-enzyme-antibody functionalized gold nanoflowers as an electrochemical detection label [14]. However, both electrochemical biosensing approaches for OFL encounter a complicated fabrication process. As a comparison, the reported sensing strategies for OFL are listed in Table 3. Overall, our electrochemical aptasensing strategy offers several advantages compared to the reported electrochemical (bio)sensors for the detection of OFL: (1) the fabrication process is low-cost, fast and straightforward, (2) long-term stability, i.e. it can be used over a month with only a slight decrease in signal, (3) easy regeneration and reuse for multiple assays and (4) high sensitivity (1 nM) and superior selectivity.

4. Conclusion

A joint action of a glassy carbon electrode, gold nanoparticles, aptamers and electrochemistry comprise a new sensing strategy for low molecular weight compounds. We employed gold nanoparticles as a signal amplification platform for improved immobilization of selected ssDNA aptamers as highly specific recognition elements for ofloxacin. Firstly, the gold nanoparticles, which exhibit high electron transfer, large surface area, and strong probe immobilization abilities have been integrated in the construction of the aptasensor. These nanoparticles have been covalently attached to the surface of the electrode increasing the stability of the proposed aptasensor toward electrochemical stresses. Highly specific OFL binding aptamers which were selected through the Capture-SELEX procedure were employed as biorecognition element. Through these multiple effects and using this nanomaterial-based aptamer sensing strategy, we could determine OFL within a linear range of 5×10^{-8} to 2×10^{-5} M and a very low detection limit of 1×10^{-9} M. The proposed aptasensing device offers several advantages such as (a) low detection limit; (b) simple experimental procedure; (c) label-free aptadetection; (d) high stability and selectivity; (e) ability to sense OFL in real environmental samples which demonstrates it applicability for environmental monitoring.

Acknowledgment

This work was financially supported by the University of Antwerp (BOF), the Research Foundation - Flanders (FWO) and the Hercules Foundation. S. P. is thankful to UA for DOCPRO financial support. C.R. and B.S. acknowledge funding by the Federal Ministry of Education and Research (BMBF) under contract no. 03X0094B.

References

[1] A.T. Nair, Pharmaceuticals in Environment: A review on its effect, Res. J. Chem. Sci. 2 (2012) 103-105.
[2] C.H. Huang, J.E. Renew, K.L. Smeby, K. Pinkston, D.L. Sedlak, Assessment of potential antibiotics contaminants in water and preliminary occurance analysis, J. Contemp. Water Res. Educ. 120 (2001) 30-40.
[3] S. Kim, D.S. Aga, Potential ecological and human health impacts of antibiotics and antibiotic-resistant bacteria from wastewater treatment plants, J. Toxicol. Environ. Health B 10 (2007) 559-573.
[4] K. Kümmerer, Significance of antibiotics in the environment, J. Antimicrob. Chemother. 52 (2003) 5-7.
[5] R. Hirsch, T. Ternes, K. Haberer, K.-L. Kratz, Occurrence of antibiotics in the aquatic environment, Sci. Total Environ. 225(1999) 109-118.
[6] K. He, A.D. Soares, H. Adejumo, M. McDiarmid, K. Squibb, L. Blaney, Detection of a wide variety of human and veterinary fluoroquinolone antibiotics in municipal wastewater and wastewater-impacted surface water, J. Pharm. Biomed. Anal. 106 (2015) 136-143.
[7] L.R. Peterson, Quinolone molecular structure-activity relationships: what we have learned about improving antimicrobial activity, Clin. Infect. Dis. 33 (2001) 180-186.
[8] J. Monk, D. Campoli-Richards, Ofloxacin. A review of its antibacterial activity, pharmacokinetic properties and therapeutic use, Drugs 33 (1987) 346-391.
[9] S. Zang, Y. Liu, M. Lin, J. Kang, Y. Sun, H. Lei, A dual amplified electrochemical immunosensor for ofloxacin: Polypyrrole film-Au nanocluster as the matrix and multi-enzyme-antibody functionalized gold nanorod as the label, Electrochim. Acta 90 (2013) 246-253.
[10] Z. He, S. Zang, Y. Liu, Y. He, H. Lei, A multi-walled carbon nanotubes-poly(l-lysine) modified enantioselective immunosensor for ofloxacin by using multi-enzyme-labeled gold nanoflower as signal enhancer, Biosens. Bioelectron. 73 (2015) 85-92.
[11] G. Zhou, J. Pan, Polarographic and voltammetric behaviour of ofloxacin and its analytical application, Anal. Chim. Acta 307 (1995) 49-53.
[12] F. Tan, Q. Zhao, F. Teng, D. Sun, J. Gao, X. Quan, et al., Molecularly imprinted polymer/mesoporous carbon nanoparticles as electrode sensing material for selective detection of ofloxacin, Mater. Lett. 129 (2014) 95-97.
[13] T.S. Chen, K. L. Huang, J.-L. Chen, An electrochemical approach to simultaneous determination of acetaminophen and ofloxacin, Bull. Environ. Contam. Toxicol. 89 (2012) 1284-1288.
[14] R. Gulaboski, B. Jordanoski, square wave voltammetry of ofloxacin, Bull. Chem. Technol. Macedonia 19 (2000) 177-181.
[15] F. Zhang, S. Gu, Y. Ding, L. Li, X. Liu, Simultaneous determination of ofloxacin and gatifloxacin on cysteic acid modified electrode in the presence of sodium dodecyl benzene sulfonate, Bioelectrochem. 89 (2013) 42-49.
[16] C. Yang, Y. Xu, C. Hu, S. Hu, Voltammetric detection of ofloxacin in human urine at a congo red functionalized water-soluble carbon nanotube film electrode, Electroanal. 20 (2008) 144-149.
[17] F.A. El-Yazbi, Spectrophotometric and spectrofluorimetric determination of ofloxacin, Spectrosc. Lett. 25 (1992) 279-291.
[18] K.N. Prashanth, K. Basavaiah, M.S. Raghu, Simple and selective spectrophotometric determination of ofloxacin in pharmaceutical formulations using two sulphonphthalein acid dyes, ISRN Spectrosc. 2013 (2013) 1-9.
[19] D. Fabre, F. Bressolle, J.M. Kinowski, O. Bouvet, F. Paganin, M. Galtier, A reproducible, simple and sensitive HPLC assay for determination of ofloxacin in plasma and lung tissue. Application in pharmacokinetic studies, J. Pharm. Biomed. Anal. 12 (1994) 1463-1469.
[20] V.F. Samanidou, C.E. Demetriou, I.N. Papadoyannis, direct determination of four fluoroquinolones, enoxacin, norfloxacin, ofloxacin, and ciprofloxacin, in pharmaceuticals and blood serum by HPLC, Anal. Bioanal. Chem. 375 (2003) 623-629.
[21] R. Stoltenburg, C. Reinemann, B. Strehlitz, SELEX-A (r)evolutionary method to generate high-affinity nucleic acid ligands, Biomol. Eng. 24 (2007) 381-403.
[22] C. Reinemann, U. Freiin von Fritsch, S. Rudolph, B. Strehlitz, Generation and characterization of quinolone-specific DNA aptamers suitable for water monitoring, Biosens. Bioelectron. 77 (2016) 1039-1047.

[23] R. Stoltenburg, N. Nikolaus, B. Strehlitz, Capture-SELEX: Selection of DNA aptamers for aminoglycoside antibiotics, J. Anal. Methods Chem. 2012 (2012) 14.
[24] S. Song, L. Wang, J. Li, J. Zhao, C. Fan, Aptamer-based biosensors. Trends Anal. Chem. 27 (2008) 108–117.
[25] K. M. Song, S. Lee, C. Ban, Aptamers and their biological applications, Sensors 12 (2012) 612-631.
[26] N. Xu, Q. Wang, J. Lei, L. Liu, H. Ju, Label-free triple-helix aptamer as sensing platform for "signal-on" fluorescent detection of thrombin, Talanta 132 (2015) 387-391.
[27] S. Li, D. Chen, Q. Zhou, W. Wang, L. Gao, J. Jiang, et al., A general chemiluminescence strategy for measuring aptamer–target binding and target concentration, Anal. Chem. 86 (2014) 5559-5566.
[28] J.E. Smith, D.K. Griffin, J.K. Leny, J.A. Hagen, J.L. Chávez, N. Kelley-Loughnane, Colorimetric detection with aptamer-gold nanoparticle conjugates coupled to an android-based color analysis application for use in the field, Talanta 121 (2014) 247-255.
[29] Z. Li, L. Sun, Y. Zhao, L. Yang, H. Qi, Q. Gao, Z. Chengxiao, Electrogenerated chemiluminescence aptasensor for ultrasensitive detection of thrombin incorporating an auxiliary probe, Talanta 130(2014) 370-376.
[30] T. Hianik, J. Wang, Electrochemical aptasensors – recent achievements and perspectives, Electroanal. 21 (2009) 1223-1235.
[31] F.J. Hernandez, V.C. Ozalp, Graphene and other nanomaterial-based electrochemical aptasensors, Biosens. 2 (2012) 1-14.
[32] A. Sassolas, L.J. Blum, B.D. Leca-Bouvier, Electrochemical aptasensors, Electroanal. 21 (2009) 1237-1250.
[33] B. Wei, N. Liu, J. Zhang, X. Ou, R. Duan, Z. Yang, et al., Regulation of DNA self-assembly and DNA hybridization by chiral molecules with corresponding biosensor applications, Anal. Chem. 87 (2015) 2058-2062.
[34] M. Vestergaard, K. Kerman, E. Tamiya, An overview of label-free electrochemical protein sensors, Sensors 7 (2007) 3442-3458.
[35] B. Strehlitz, N. Nikolaus, R. Stoltenburg, Protein detection with aptamer biosensors, Sensors 8 (2008) 4296-4307.
[36] H. Liu, S. Xu, Z. He, A. Deng, J.-J. Zhu, Supersandwich cytosensor for selective and ultrasensitive detection of cancer cells using aptamer-DNA concatamer-quantum dots probes, Anal. Chem. 85 (2013) 3385-3392.
[37] B. Li, Y. Du, H. Wei, S. Dong, Reusable, label-free electrochemical aptasensor for sensitive detection of small molecules, Chem. Commun. (2007) 3780-3782.
[38] S. Pilehvar, T. Dierckx, R. Blust, T. Breugelmans, K. De Wael, An electrochemical impedimetric aptasensing platform for sensitive and selective detection of small molecules such as chloramphenicol, Sensors 14 (2014) 12059-12069.
[39] G. Wang, X. He, B. Wang, X. Zhang, L. Wang, Electrochemical amplified detection of Hg2+ based on the supersandwich DNA structure, Analyst 137 (2012) 2036-2038.
[40] T. Yuan, Z. Liu, L. Hu, L. Zhang, G. Xu, Label-free supersandwich electrochemiluminescence assay for detection of sub-nanomolar Hg^{2+}, Chem. Commun. 47 (2011) 11951-11953.
[41] R. Sharma, K.V. Ragavan, M.S. Thakur, K.S.M.S. Raghavarao, Recent advances in nanoparticle based aptasensors for food contaminants, Biosens. Bioelectron. 74 (2015) 612-627.
[42] G. Wang, Y. Wang, L. Chen, J. Choo, Nanomaterial-assisted aptamers for optical sensing, Biosens. Bioelectron. 25 (2010) 1859-1868.
[43] Y.S. Kim, J.H. Kim, I.A. Kim, S.J. Lee, J. Jurng, M.B. Gu, A novel colorimetric aptasensor using gold nanoparticle for a highly sensitive and specific detection of oxytetracycline, Biosens. Bioelectron. 26 (2010) 1644-1649.
[44] W. Bai, C. Zhu, J. Liu, M. Yan, S. Yang, A. Chen, Gold nanoparticle–based colorimetric aptasensor for rapid detection of six organophosphorous pesticides, Environ. Toxicol. Chem. 34 (2015) 2244-2249.
[45] C. Zhu, G. Yang, H. Li, D. Du, Y. Lin, Electrochemical sensors and biosensors based on nanomaterials and nanostructures, Anal. Chem. 87 (2015) 230-249.
[46] J.M. Pingarrón, P. Yáñez-Sedeño, A. González-Cortés, Gold nanoparticle-based electrochemical biosensors, Electrochim. Acta 53 (2008) 5848-5866.
[47] K.J. Huang, Y. –J. Liua, Y. –M. Liua, L.-L. Wanga, Molybdenum disulfide nanoflower-chitosan-Au nanoparticles composites based electrochemical sensing platform for bisphenol A determination, J. Hazard. Mater. 276 (2014) 207-215.
[48] L. –X. Fang, K. –J. Huang, , Y. Liu, Novel electrochemical dual-aptamer-based sandwich biosensor using molybdenum disulfide/carbon aerogel composites and Au nanoparticles for signal amplification, Biosens. Bioelectron. 71 (2015) 171–178
[49] X. Li, H. Qi, L. Shen, Q. Gao, C. Zhang, Electrochemical aptasensor for the determination of cocaine incorporating gold nanoparticles modification, Electroanal. 20 (2008) 1475-1482.
[50] H. Xu, X. Mao, Q. Zeng, S. Wang, A.-N. Kawde, G. Liu, Aptamer-functionalized gold nano particles as probes in a dry-reagent strip biosensor for protein analysis, Anal. Chem. 81 (2009) 669-675.
[51] F. Shahdost-fard, A. Salimi, S. Khezrian, Highly selective and sensitive adenosine aptasensor based on platinum nanoparticles as catalytical label for amplified detection of biorecognition events through H_2O_2 reduction, Biosens. Bioelectron. 53 (2014) 355-362.
[52] B. Wei, J. Zhang, H. Wang, F. Xia, A new electrochemical aptasensor based on a dual-signaling strategy and supersandwich assay, Analyst 141 (2016) 4313-4318.
[53] K.J. Huang, H.L. Shuai, Y.X. Chen, Layered molybdenum selenide stacking flower-like nanostructure coupled with guanine-rich DNA sequence for ultrasensitive ochratoxin A aptasensor application, Sensors Actuat. B Chem. 225 (2016) 391-397.
[54] X. Li, H. Fu, Y. He, Q. Zhai, J. Guo, K. Qing, et al., Electrochemical aptasensor for rapid and sensitive determination of salmonella based on target-induced strand displacement and gold nanoparticle amplification, Anal. Lett. (2016) 1-30.
[55] K.E. Sapsford, W.R. Algar, L. Berti, K.B. Gemmill, B.J. Casey, E. Oh, et al., Functionalizing nanoparticles with biological molecules: developing chemistries that facilitate nanotechnology, Chem. Rev. 113 (2013) 1904-2074.

[56] M. Roushani, F. Shahdost-fard, Fabrication of an ultrasensitive ibuprofen nanoaptasensor based on covalent attachment of aptamer to electrochemically deposited gold-nanoparticles on glassy carbon electrode, Talanta 144 (2015) 510-516.
[57] P. Gobbo, S. Ghiassian, M. Hesari, K.G. Stamplecoskie, N. Kazemi-Zanjani, F. Lagugne-Labarthet, et al., Electrochemistry of robust gold nanoparticle-glassy carbon hybrids generated using a patternable photochemical approach, J. Mater. Chem. 22 (2012) 23971-23980.
[58] F. Patolsky, E. Katz, I. Willner, Amplified DNA detection by electrogenerated biochemiluminescence and by the catalyzed precipitation of an insoluble product on electrodes in the presence of the doxorubicin intercalator, Angew. Chem. Int. Ed. 41 (2002) 3398-3402.
[59] L. Zhang, X. Jiang, E. Wang, S. Dong, Attachment of gold nanoparticles to glassy carbon electrode and its application for the direct electrochemistry and electrocatalytic behavior of hemoglobin, Biosens. Bioelectron. 21(2005) 337-345.
[60] S. Balamurugan, A. Obubuafo, R.L. McCarley, S.A. Soper, D.A. Spivak, Effect of linker structure on surface density of aptamer monolayers and their corresponding protein binding efficiency, Anal. Chem. 80 (2008) 9630-9634.
[61] X. Wang, A. Jiang, T. Hou, F. Li, A sensitive and versatile "signal-on" electrochemical aptasensor based on a triple-helix molecular switch, Analyst 139 (2014) 6272-6278.
[62] S. Guo, E. Wang, Synthesis and electrochemical applications of gold nanoparticles, Anal. Chim. Acta 598 (2007) 181–192.
[63] M. Rizk, F. Belal, F.A. Aly, N.M. El-Enany, Differential pulse polarographic determination of ofloxacin in pharmaceuticals and biological fluids, Talanta 46 (1998) 83-89.
[64] J.I. Gowda, S.T. Nandibewoor, Electrochemical behavior of paclitaxel and its determination at glassy carbon electrode, Asian J. Pharm. Sci. 9 (2014) 42-49.
[65] J.M. Kauffmann, J.C. Vire, G.J. Patriarche, L.J. Nunez-Vergara, J.A. Squella, Voltammetric oxidation of trazodone, Electrochim. Acta 32 (1987) 1159-1162.
[66] H. Shin, C. Kang, Adhesion of gold nanoparticles on an electrochemically pretreated glassy carbon electrode, Anal. Sci. 19 (2003) 1667-1670.
[67] A. Erdem, Nanomaterial-based electrochemical DNA sensing strategies, Talanta, 74 (2007) 318-325.
[68] J.A. Harnisch, A.D. Pris, M.D. Porter, Attachment of gold nanoparticles to glassy carbon electrodes via a mercaptobenzene film, J. Am. Chem. Soc. 123 (2001) 5829-5830.
[69] J. Liu, L. Cheng, B. Liu, S. Dong, Covalent modification of a glassy carbon surface by 4-aminobenzoic acid and its application in fabrication of a polyoxometalates-consisting monolayer and multilayer films, Langmuir 16 (2000) 7471-7476.
[70] T. Hezard, K. Fajerwerg, D. Evrard, V. Collière, P. Behra, P. Gros, Gold nanoparticles electrodeposited on glassy carbon using cyclic voltammetry: Application to Hg(II) trace analysis, J. Anal. Chem. 664 (2012) 46-52.
[71] G.-Y. Kim, J. Shim, M.-S. Kang, S.-H. Moon, Optimized coverage of gold nanoparticles at tyrosinase electrode for measurement of a pesticide in various water samples, J. Hazard. Mater. 156 (2008) 141-147.
[72] G. Yang, Y. Shen, M. Wang, H. Chen, B. Liu, S. Dong, Copper hexacyanoferrate multilayer films on glassy carbon electrode modified with 4-aminobenzoic acid in aqueous solution, Talanta 68 (2006) 741-747.
[73] J.-M. You, D. Kim, S.K. Kim, M.-S. Kim, H.S. Han, S. Jeon, Novel determination of hydrogen peroxide by electrochemically reduced graphene oxide grafted with aminothiophenol–Pd nanoparticles, Sensors Actuat. B Chem. 178 (2013) 450-457.
[74] S. Pilehvar, J. Ahmad Rather, F. Dardenne, J. Robbens, R. Blust, K. De Wael, Carbon nanotubes based electrochemical aptasensing platform for the detection of hydroxylated polychlorinated biphenyl in human blood serum, Biosens. Bioelectron. 54 (2014) 78-84.
[75] X. Wang, A. Jiang, T. Hou, F. Li, A sensitive and versatile "signal-on" electrochemical aptasensor based on a triple-helix molecular switch, Analyst 139 (2014) 6272-6278.
[76] A.B. Steel, T.M. Herne, M.J. Tarlov, Electrochemical quantitation of DNA immobilized on gold, Anal. Chem. 70 (1998) 4670-4677.
[77] X. Li, L. Shen, D. Zhang, H. Qi, Q. Gao, F. Ma, et al., Electrochemical impedance spectroscopy for study of aptamer–thrombin interfacial interactions, Biosens. Bioelectron. 23 (2008) 1624-1630.
[78] H. Han, J.-Z. Li, X.-Z. Pang, Electrochemical sensor using glassy carbon electrode modified with HPMαFP/Ppy/GCE composite film for determination of ofloxacin, Int. J. Electrochem. Sci. 8 (2013) 9060-9070.
[79] S. Pilehvar, J. Mehta, F. Dardenne, J. Robbens, R. Blust, K. De Wael, Aptasensing of chloramphenicol in the presence of its analogues: reaching the maximum residue limit, Anal. Chem. 84 (2012) 6753-6758.
[80] J. Wang, G. Rivas, M. Jiang, X. Zhang, Electrochemically induced release of DNA from gold yltramicroelectrodes, Langmuir 15 (1999) 6541-6545.
[81] P.G. Vijaya, Y.S. Bafana, S.Y. Deshapande, M.R. Vyas, A.V. Bhosale, Validated stability-indicating HPLC method for simultanous estimation of Ofloxacin and Satranidazole from pharmacutical dosage from International, Int. J. Appl. Biol. Pharm.Tech. 1 (2010) 1220-1229.
[82] Y. Liu, N. Tuleouva, E. Ramanculov, A. Revzin, Aptamer-based electrochemical biosensor for interferon gamma detection, Anal. Chem. 82 (2010) 8131-8136.
[83] P. Wang, Y. Wan, Y. Su, S. Deng, S. Yang, Ultrasensitive electrochemical aptasensor based on surface-initiated enzymatic polymerization, Chinese J. Chem. 34 (2016) 337-341.

Sanaz Pilehvar is currently working as a Post Graduate researcher in the Antwerp X-ray analysis, Electrochemistry and Speciation (AXES) Group, Chemistry Department at the University of Antwerp, Belgium. She received her Ph.D. and M.Sc. in Analytical Chemistry from University of Antwerp and Tehran Polytechnique in 2016 and 2011 and B.Sc. in Applied Chemistry from Tabriz University in 2009. Currently, she is working on the development of new strategies for electrochemical aptasensing of environmentally important molecules.

Christine Reinemann received her diploma as biotechnology engineer from Anhalt University of Applied Sciences, Köthen, Germany in 1992 and her Ph.D. degree in biochemistry from University of Leipzig, Germany in 2007. Currently, she is working as a Senior Laboratory Scientist in Aptamer Group Ltd., York, UK. Her scientific interests focus on the selection, characterisation and application of aptamers.

Fabio Bottari received his Master Degree in Chemical Science for Conservation and Restoration in 2012 from the University Cà Foscari of Venice. He attended a Masters course in Food Quality and Safety at the University of Padua in 2013. Currently, he is working as a PhD student in the Antwerp X-ray analysis, Electrochemistry and Speciation (AXES) Group, Chemistry Department at the University of Antwerp, Belgium.

Els Vanderleyden received her M.S. and Ph.D. degree respectively in Biomedical Engineering and Chemistry from Ghent University, Belgium in 2003 and 2010. Currently, she is active as senior researcher at Ghent University (Belgium). Her scientific interests focus on polymer synthesis, polymer coatings and biomaterials.

Sandra Van Vlierberghe received her M.S. and Ph.D. degree in Chemistry from Ghent University, Belgium in 2003 and 2008, respectively. Currently, she holds a professorship at Vrije Universiteit Brussel and University of Antwerp (Belgium), while she is appointed associate professor at Ghent University. Her scientific interests focus on (bio)polymer synthesis and processing, biomaterials, photonics and optical applications.

Beate Strehlitz received her diploma in Electrotechnology/Electrochemistry from Technical University Ilmenau, Germany in 1985 and her Ph.D. degree in Natural Sciences as Doctor of Engineering from University Witten/Herdecke, Germany in 1995. Currently, she is working as a Senior Scientist at Helmholtz-Centre for Environmental Research, Leipzig, Germany. Her scientific interests focus on biotechnology, biosensors, aptamers and bioelectrochemistry.

Ronny Blust is Professor and spokesperson of the Systemic Physiological and Ecotoxicological Research (Sphere) Group, Biology Department at the University of Antwerp, Belgium. He received his PhD in Sciences/Biology in 1988 at the University of Antwerp. His group performs fundamental and applied research concerning key issues in environmental and adaptational biology.

Karolien De Wael is Professor and spokesperson of the Antwerp X-ray analysis, Electrochemistry and Speciation (AXES) Group, Chemistry Department at the University of Antwerp, Belgium. She received her Ph.D. from the University of the Ghent, Belgium in 2001. During her Ph.D. she focused on the electrochemical immobilization of transition metal ion phthalocyanines and porphyrins on electrode surfaces in order to catalyze specific reactions. She worked as FWO-postdoctoral fellow at the University of Ghent, Belgium up to March 2011 and her research were focused on the immobilization of redox proteins on electrode surfaces.

Figure captions:

Figure 1: Electrooxidation of ofloxacin.

Figure 2. (A) SEM image of bare GCE (a), and gold colloidal particles adsorbed on ATP/ABA/GCE (b) and GCE (c), (B) XPS spectra of (a) ABA/GCE, (b) ATP/ABA/GCE, (c) AuNPs/ABA/ATP/GCE and (d) AuNPs/ATP/ABA/GCE after being rinsed with a I-B buffer solution and (C) Cyclic voltammogram of AuNPs/ATP/ABA/GCE (solid line (curve 1), 1^{th} scan; solid line (curve 2), 2^{th} scan) and AuNPs/GCE (dotted line (curve 3), 1^{th} scan; dotted line (curve 4), 2^{th} scan) modified GC electrode in 0.1 M KCl at 0.05 Vs^{-1}.

Figure 3. Nyquist diagrams of the designed aptasensor at different modification stages (1) GCE, (2) ABA/GCE, (3) ATP/ABA/GCE, (4)AuNPs/ATP/ABA/AuNPs, (5)APT/AuNPs/ATP/ABA/GCE, and (6)MCH/APT/AuNPs/ATP/ABA/GCE. The measurements were carried out in 0.1 M KCl solution containing 1×10^{-3} M $Fe(CN)_6^{-3}/Fe(CN)_6^{-4}$, an amplitude of 10 mV and a frequency range of 1 Hz to 10 kHz. The inset shows the equivalent electrical circuit.

Figure 4. (A) Cyclic voltammograms of bare GCE (dotted line 1), AuNPs/ATP/ABA/GCE (green line 2), APT/AuNPs/ATP/ABA/GCE (red line 4) incubated with 5×10^{-5} M OFL solution and APT/AuNPs/ATP/ABA/GCE (brown dashed line 3) in blank I-B buffer solution, (B) cyclic voltammograms obtained at ABA/GCE (dashed line 1), ATP/ABA/GCE (dotted line 2) in a blank I-B buffer solution and ABA/GCE (green solid line 3), ATP/ABA/GCE (black solid line 4) incubated in 5×10^{-5} M OFL solution.

Figure 5. The DPV peak current of OFL versus (A) pH, (B) incubation time of the aptasensing device with 1×10^{-6} M OFL and (C) aptamer concentration.

Figure 6. DPV response (ΔI) of APT/AuNPs/ATP/ABA/GCE in the presence of 1×10^{-6} mol L^{-1} OFL (a), 1×10^{-6} mol L^{-1} CAP (b), 1×10^{-6} M NAL (c), 1×10^{-6} M POFL (d), and at RP-ssDNA/AuNPs/ATP/ABA/GCE in the presence of 1×10^{-6} M OFL (e).

Figure 7. DPV response of APT/AuNPs/ATP/ABA corresponding to the analysis of OFL with different concentrations: (a) 1×10^{-7} M, (b) 5×10^{-7} M, (c) 1×10^{-6} M, (d) 5×10^{-6} M, (e) 1×10^{-5} M and (f) 2×10^{-5} M (A). Calibration curve corresponding to the DPV peak currents measured as a function of OFL concentration (B). The inset is the calibration curve for lower concentrations.

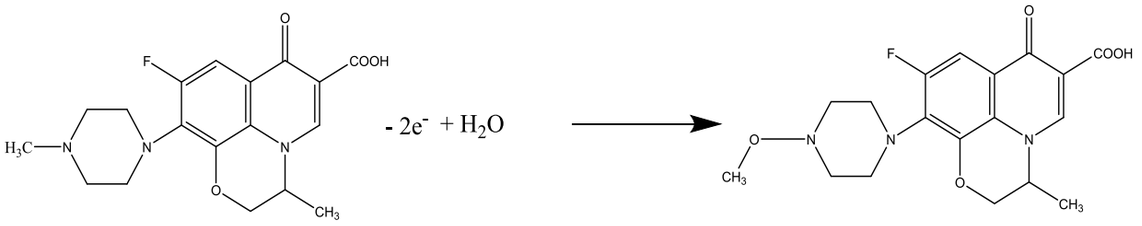

Figure 1

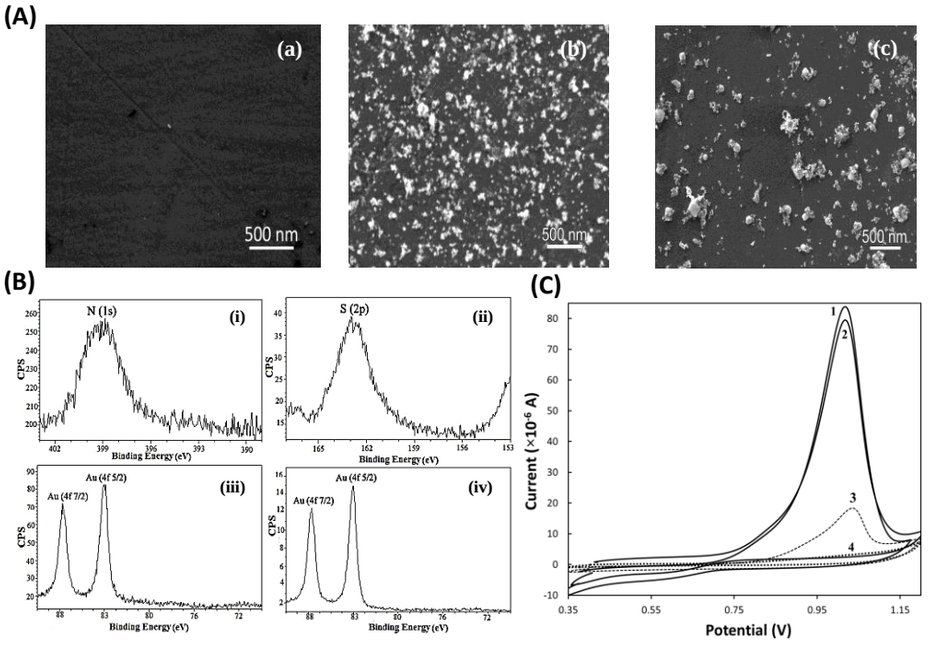

Figure 2

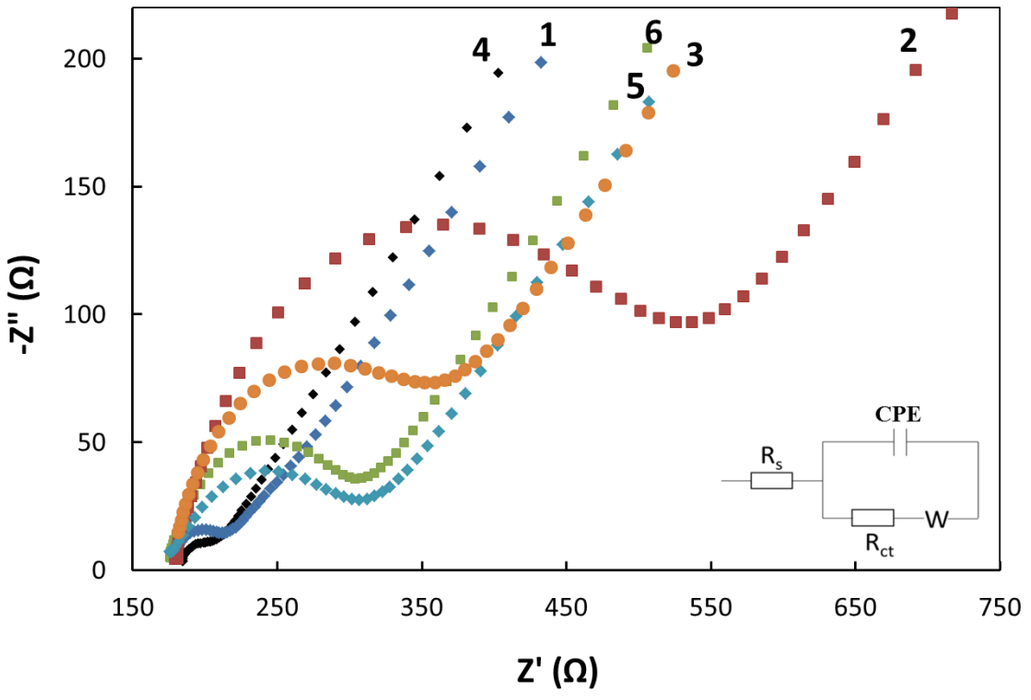

Figure 3

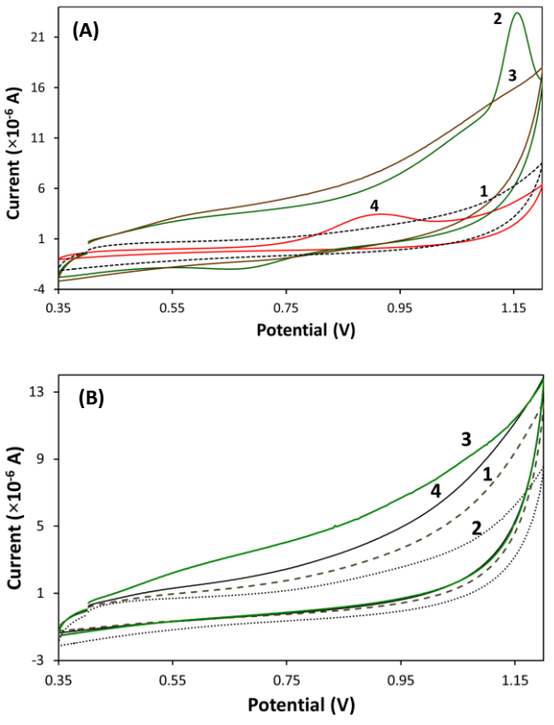

Figure 4

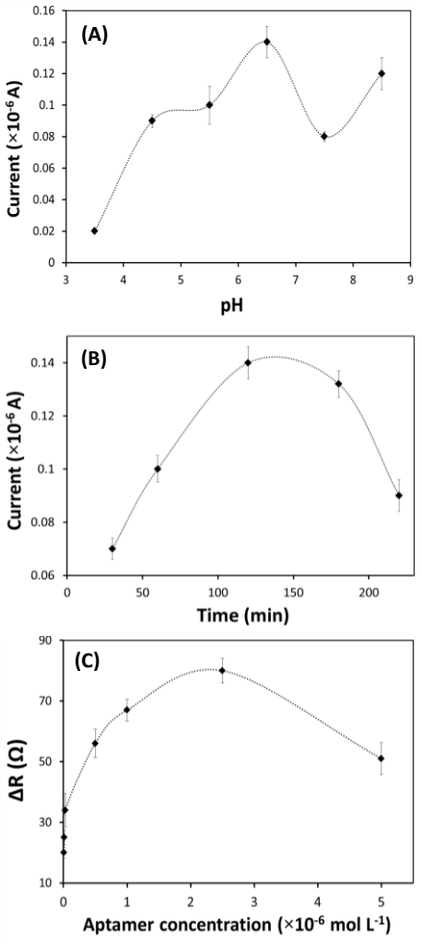

Figure 5

\

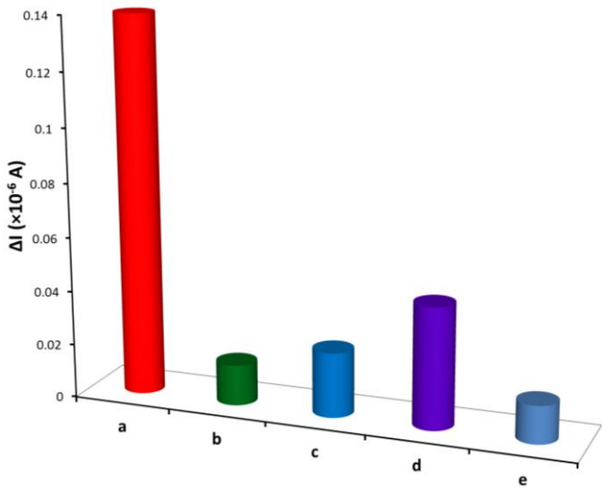

Figure 6

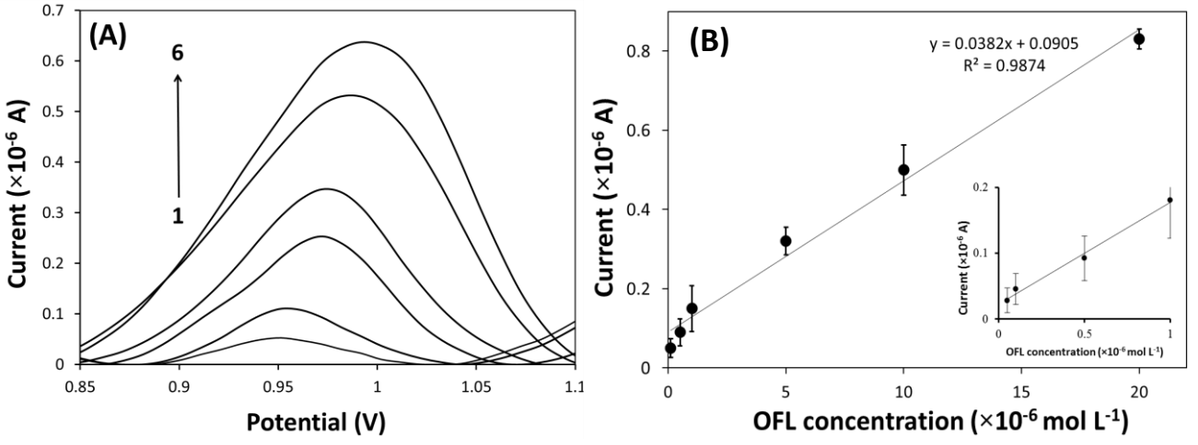

Figure 7

Scheme 1: Schematic representation of the construction of the aptasensing electrode surface for OFL.

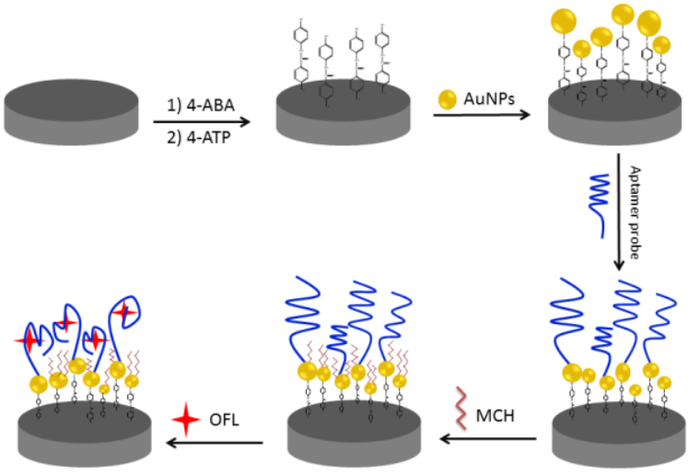

Scheme 1

Table 1. Values of the circuit elements obtained by fitting the experimental data from Figure 3 to the circuit model shown in the inset of Figure 3.

Electrode	R_s (Ω)	C_{dl} (nF)	R_{ct} (Ω)	W (μMho)	χ^2
ıre GCE	180	712	60	197	0.0004
ȝA/GCE	181	820	360	167	0.0008
ΓP/ABA/GCE	180	860	120	120	0.0001
ıNPs/ATP/ABA/GCE	180	915	20	121	0.0005
ƿT/AuNPs/ATP/ABA/GCE	185	2200	170	84	0.01
CH/APT/AuNPs/ABA/GCE	180	2350	270	72	0.015

Table 2. Results on the detection of OFL in spiked tap water and the effluent of sewage plant samples by the standard addition method and comparison between the developed electrochemical aptasensor in this study and an assay using UV-Vis spectrometric method. Mean values and RSDs were from three independent experiments.

		Electrochemical Aptasensor			UV-Vis spectrophotometry		
Sample	**Added ($\times10^{-6}$ M)**	**Found ($\times10^{-6}$ M)**	**Recovery %**	**RSD %**	**Found ($\times10^{-6}$ M)**	**Recovery %**	**RSD %**
Spiked plant sewage water	0	0	-	1.12	0	-	0.55
	0.5	0.46	93.6	6.73	0.49	98	4.83
Spiked tap water	0	0	-	1.84	0	-	0.51
	0.5	0.48	96	4.52	0.51	102	3.72

Table 3. Comparison between different electrochemical techniques used for the detection of ofloxacin.

Electrode	LOD (M)	Linear range (M)	Detection time	Reference
Au nanoparticle/Aptamer modified glassy carbon electrode	1×10^{-9}	5×10^{-8}-2×10^{-5}	24 s	This work
Au nanocluster/Polypyrrole modified glassy carbon electrode and gold nano horseradish peroxidase/horseradish peroxidase-secondary antibody	8.2×10^{-11}	2×10^{-10}-1.1×10^{-8}	60 min	[13]
Multi-walled carbon nanotubes-poly(l-lysine) modified immunosensor and multi-enzyme-labeled gold nanoflower	0.15*	0.26 - 25.6 *	60 min	[14]
Mercury drop electrode	4×10^{-6}	8×10^{-4}-2×10^{-5}	-	[15]
poly(L-serine) film-modified glassy carbon electrode	1.6×10^{-7}	1×10^{-5}-1×10^{-4}	-	[16]
Molecularly imprinted polymer and mesoporous carbon nanoparticle modified glassy carbon electrode	8×10^{-8}	0.5-1×10^{-4}	6 min	[17]
Mercury drop electrode	4×10^{-8}	1-10×10^{-7}	90 s	[18]
Cysteic acid modified carbon paste electrode	2×10^{-8}	0.06-1×10^{-5}	-	[18]
Congo Red functionalized multiwalled carbon nanotubes modified glassy carb electrode	9×10^{-9}	5×10^{-8}-3×10^{-5}	350 s	[19]

*ng/mL